
**MAGNETISM
AND FERROELECTRICITY**

Spin-Reorientational Phase Transition in the Basal Plane in an α -Fe₂O₃ : (Ga, Dy) Crystal

G. S. Patrin^{*, **}, E. V. Eremin^{}, and A. V. Shabalin^{*}**

^{*}*Krasnoyarsk State University, Krasnoyarsk, 660041 Russia*

^{**}*Kirenskii Institute of Physics, Siberian Division, Russian Academy of Sciences,
Akademgorodok, Krasnoyarsk, 660036 Russia*

e-mail: pat@iph.krasnoyarsk.su

Received March 14, 2000

Abstract—A spin-reorientational phase transition in the basal plane, which was experimentally observed earlier, is explained in terms of a model in which the crystalline Fe-ion matrix is considered as a continuum, while dopant Dy ions are treated as quasi-Ising ions. The transition is established to be due to the Fe-subsystem anisotropy competing with that of the rare-earth subsystem. © 2000 MAIK “Nauka/Interperiodica”.

INTRODUCTION

Magnetic compounds containing rare-earth (RE) elements differ widely in their observed properties [1]. Due to special features of the electronic structure of RE ions, the characteristic properties of these ions are most pronounced at low temperatures, where fluctuation interactions are frozen out, as a rule, and the effects of interest can be observed without hindrance. In individual cases, even a low RE-ion concentration produces marked changes in the magnetic properties.

Hematite crystals are convenient for studying induced anisotropic interactions, because almost all features of the temperature dependence of the latter are determined by the balance between magnetic anisotropies that differ in nature but make nearly equal contributions. It is well known [2] that adding several percent of $3d$ or diamagnetic ions causes the Morin transition temperature to shift to the low-temperature region $T < 4.2$ K. The authors have found that dopant RE ions impart new, hitherto unobserved properties to hematite crystals. For instance, the addition of several percent of Tb ions to a hematite crystal containing 4 at. % Ga restores the uniaxial antiferromagnetic state [3], while introducing the same amount of Dy ions induces a spin-reorientational transition in the basal plane [4].

In this paper, earlier reported experimental dependences of the magnetic-resonance parameters in the vicinity of the phase transition in α -Fe₂O₃ : (Ga, Dy) are explained theoretically.

1. MODEL

First of all, we will discuss the facts that form the basis for an impurity-center model and its interaction with the host crystal. Experimentally, it was found [4] that adding several atomic percent of Dy ions does not distort the crystal lattice markedly, which is indicated

by a virtually hexagonal magnetic anisotropy at temperatures $T > 6$ K. Above the spin-reorientational phase transition temperature T_{ph} , the easy magnetization axis has the same direction in both dysprosium-doped and undoped crystals. Also, earlier EPR studies revealed [5] that, in an isomorphic α -Al₂O₃ crystal, dopant RE ions occupy Al sites with no change in their local symmetry. In addition, it is known [6] that, at temperatures $T < 300$ K, the magnetization of hematite is virtually independent of temperature and all changes in the shape of a microwave signal are mainly due to the change in the magnetic-resonance linewidth. In our case, the intensity of an antiferromagnetic resonance (AFMR) signal, which is defined as the area under the curve of microwave absorption, is the same everywhere over the temperature range investigated (except for the phase transition region). This means that the magnetic-moment component of the Fe-ion system lies in the basal plane of the crystal (because it is this component that determines the intensity of the AFMR signal [7]) and is temperature independent, and, therefore, the magnetic moment of Dy ions also lies in the basal plane all the time.

The trivalent Dy ion has a $4f^9$ electron configuration and its ground state is a ${}^6H_{15/2}$ multiplet [8]. The crystal field of low symmetry splits this multiplet into a number of Kramers doublets, which are further split by the exchange field. Because the crystal-field splitting of electron f states corresponds to the case of a weak crystal field, the amounts of splitting will differ only slightly in different oxide compounds if the local symmetry is the same in them [1]. As a basis for our model, we use the calculations performed in [9, 10]. With the parameters $A_2^0 \langle r^2 \rangle = -22$, $A_2^2 \langle r^2 \rangle = 141$, $A_4^2 \langle r^4 \rangle = 181$, $A_6^2 \langle r^6 \rangle = -108$, and $A_6^6 \langle r^6 \rangle = -57$ cm⁻¹ (under the condition that $B_4/B_6 = (1/4)F(6)/F(4)$ in the notation of [9]),

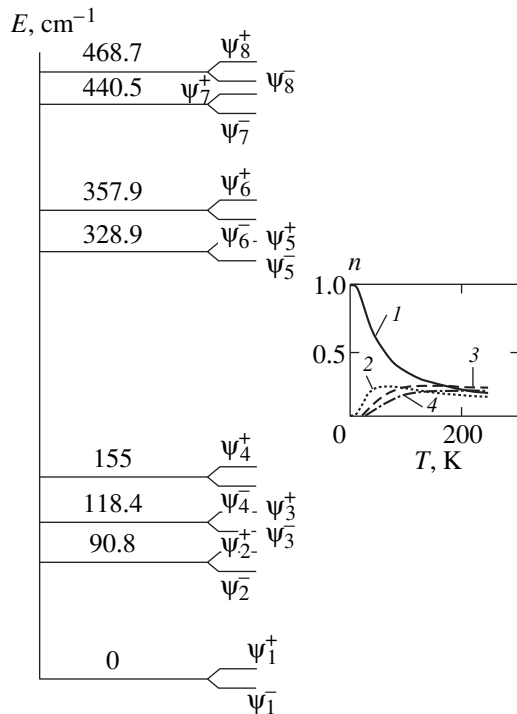


Fig. 1. Energy levels of a Dy ion in a crystal (schematic). The numbers indicate the energy in cm^{-1} . The inset shows the temperature dependence of the occupancies of the four lower energy levels.

which are typical of Dy ions in an yttrium gallium garnet host crystal, we obtain the energy levels depicted in Fig. 1 and the set of wave functions Ψ_L presented in Appendix I. Because the exchange interaction of RE ions with a host crystal is, as a rule, an order of magnitude weaker than the crystal-field splitting in magnetically ordered crystals [1], we calculate the exchange-interaction contribution to the first order in the perturbation theory. For this set of wave functions, we find the magnetic moment μ^L of an ion in each state (Appendix I). In all calculations, the exchange interaction of a Dy ion with its neighboring Fe ions is assumed to be of a quasi-Ising character [1].

We suppose that impurity ions occupy Fe^{3+} sites and are randomly distributed over 24 nonequivalent positions in the crystal. These positions are specified by a set of indices $\{k = 1, 2; s = 1, 2; t = 1, 2, \dots, 6\} = \{p\}$. The first index specifies one of the two sublattices to which the sites belong; the second indicates the angle ($\pm\alpha$) through which the axes ξ and η of the local coordinate frame are turned in the basal plane relative to the crystallographic C_2 axes (the X or Y axis of the crystal); and the third index specifies the nonequivalent angles in a given sublattice. The impurity ions occupying one of these nonequivalent positions are labeled by index q . The quantization axis Z' for Dy^{3+} ions in a local coordinate frame is taken to be aligned with the ξ axis.

In this case, the energy of an impurity ion occupying the pq position and being in the l th state has the form

$$E_{pq}^l = E_{pq}^{l0} + (-g\mathbf{H}_0 + \lambda\mathbf{M})\boldsymbol{\mu}_{Z'pq}^l, \quad (1)$$

where E_{pq}^{l0} is the crystal-field splitting, \mathbf{H}_0 is the external magnetic field, $\lambda\mathbf{M}$ is the molecular field exerted on the pq ion by the other sublattice (the intrasublattice exchange interaction can be ignored in rhombohedral antiferromagnets, because it is much weaker than the intersublattice exchange interaction), and $\boldsymbol{\mu}_{Z'pq}^l$ is the magnetic moment of an ion in the l th state. We also have $N_k = N_0/2$, $N_{ks} = N_0/4$, $N_{kst} = N_0/24$, and $\sum_{\{kstq\}} N_{kstq} = N_0$, where N_0 is the total number of impurity centers.

The total energy of the impurity subsystem is

$$F = \sum_{\{pq'l\}} n_{pq}^l E_{pq}^l - ST, \quad (2)$$

where n_{pq}^l are the equilibrium occupation numbers of the energy levels and S is the entropy of the system.

2. MAGNETIC-RESONANCE CALCULATIONS

The magnetic energy of the crystal, including the energy of the impurity subsystem, can be written as [7]

$$W = W_Z + W_E + W_D + W_{AU} + W_{AB} + W_\Delta + F. \quad (3)$$

In what follows, we consider only the case where the external magnetic field and the magnetic moments of the sublattices lie in the basal plane and, therefore, the uniaxial anisotropy energy W_{AU} makes no contribution to the low-frequency branch of the magnetic resonance. W_Δ is a contribution containing an adjustable parameter Δ and responsible for an isotropic gap in the spectrum, the term F is given by Eq. (2), while the other terms in Eq. (3) can be written in a spherical coordinate system in the form

$$W_Z = -H_0 M_0 [\cos(\varphi_H - \varphi_1) + \cos(\varphi_H - \varphi_2)],$$

$$W_E = A_E M_0^2 \cos(\varphi_1 - \varphi_2),$$

$$W_D = -A_D M_0^2 \sin(\varphi_1 - \varphi_2),$$

$$W_{AB} = A_B M_0^2 (\cos 6\varphi_1 + \cos 6\varphi_2),$$

and they are the Zeeman interaction, intersublattice interaction, Dzyaloshinskii interaction, and anisotropy energy in the basal plane, respectively. Here, M_0 is the saturation magnetization of a sublattice; φ_1 and φ_2 are the azimuthal angles of the sublattice magnetizations; φ_H is the angle between the magnetic field and the C_2 axis; A_E and A_D are the interaction constants; and A_B is the anisotropy constant.

The equilibrium values of the azimuthal angles of the sublattice magnetizations are determined from the minimum-energy condition

$$\partial W / \partial \varphi_k = 0, \quad (k = 1, 2) \quad (4)$$

with $\varphi_1 - \varphi_2 = \pi - \delta_1 - \delta_2$, where δ_k are the canting angles of the sublattices. If the sublattices are identical and impurity ions are randomly distributed over the sublattice sites, we have $\delta_1 = \delta_2 = \delta$.

From Eq. (4), the canting angle is found to be (for $\delta \ll 1$)

$$\delta \approx (H_0 + H_D - 6H_{AB} \sin 6\varphi_H - \partial F / \partial \varphi_1) / (2H_E + 36H_{AB} \cos 6\varphi_H), \quad (5)$$

where we have put $\varphi_1 = \varphi_H + \pi/2 - \delta$ at equilibrium, and H_0, H_E, H_D , and H_{AB} are the effective fields corresponding to the energy contributions in Eq. (3).

By solving the Landau–Lifshitz equations in a linear approximation, the following expression is obtained for the uniform-mode resonance field H_r of low-frequency oscillations:

$$H_r = -(H_D/2) + \{(H_D/2)^2 + (\omega/\gamma)^2 + \Delta^2 - 2H_E(36H_{AB} \cos 6\varphi_H + E_{\varphi\varphi})\}^{1/2}. \quad (6)$$

Here, ω is the microwave frequency, γ is the gyromagnetic ratio, Δ is the isotropic band gap, and $F_{\varphi\varphi}$ is the second derivative of the impurity-subsystem energy with respect to either of the φ_1 and φ_2 angles.

As is seen from Appendix I, the structure of the wave functions is such that the magnetic moment has a maximum value in the ground doublet state, whereas it is much smaller in the next and higher doublet states. Taking into account the Boltzmann factor characterizing the occupancies of excited energy levels (see the inset in Fig. 1), the calculation of $F_{\varphi\varphi}$ can be simplified by retaining only the four lower levels in the model. In this case, the magnetic contributions from the upper three doublets (next in energy after the ground doublet) can be ignored, and the levels themselves can be replaced by an effective twofold degenerate level E^* (with $\mu_{pq}^{\pm(2)} = 0$) positioned at the centroid of this group of levels. The results are not altered radically in the case of a higher degeneracy of the effective excited level. The expression for $F_{\varphi\varphi}$ thus calculated is presented in Appendix II.

Calculations are performed for the parameters $H_E = 9.7 \times 10^6$, $H_D = 21.7 \times 10^3$ Oe, $\alpha = 23.1^\circ$, $\lambda M = 3.5 \times 10^5$ Oe, $E^* = 121 \text{ cm}^{-1}$, $\mu_{pq}^{1,2} = \mp 2.83 \mu_B$, and $N_0 = 8.2 \times 10^{17} \text{ cm}^{-3}$. The temperature dependences of the anisotropy field in the basal plane and of the isotropic band gap are approximated by polynomials by using the experimental curves obtained for hematite crystals without Dy ions, $H_{AB}(T) = (4.4 - 0.011T + 3.12T^2 \times$

$$10^{-4} - 3.63T^3 \times 10^{-6} + 1.31T^4 \times 10^{-8} - 1.5T^5 \times 10^{-11}) \times 10^6 \text{ Oe and } \Delta^2(T) = (28.4 - 0.016T) \times 10^6 \text{ Oe}^2.$$

3. RESULTS AND DISCUSSION

The first feature to note is that the exchange interaction of the Fe-ion subsystem with a Dy ion has to be taken as ferromagnetic in the case under consideration, despite the exchange interaction with RE ions being antiferromagnetic in all known oxide compounds [1].

Figure 2 shows the theoretically calculated temperature dependences of the resonance field H_r for angles of $\varphi_H = 0^\circ$ and 30° (curves 1 and 2, respectively) and the experimental dependences taken from [4] (curves 3, 4). On the whole, the results are seen to agree satisfactorily with the experiment, except for the clearly defined high-temperature peak on the experimental curve 4 (which is associated with high energy levels), although the theoretical curve also shows a peak (curve 1). The reason for this discordance is that the magnetic moments in the high excited states have been taken to be zero. Nevertheless, this fact has no effect on the character of the spin-reorientational phase transition and its temperature for the given position of the energy levels. The occupancies of higher energy levels become noticeable at temperatures $T \geq 100$ K and, as the number of occupied excited levels increases, their relative contribution decreases.

Figure 3 shows the angular dependence of the resonance field calculated for different temperatures. It is seen that, for the parameters chosen, the angular dependence is changed in character near $T_{ph} \cong 12$ K; namely, the maxima and minima interchanged places, which can be interpreted as the change in sign of the magnetocrystalline anisotropy constant in the basal plane. There is some discordance between the calculated and experimental dependences, which may be due to the fact that the calculations include the experimental

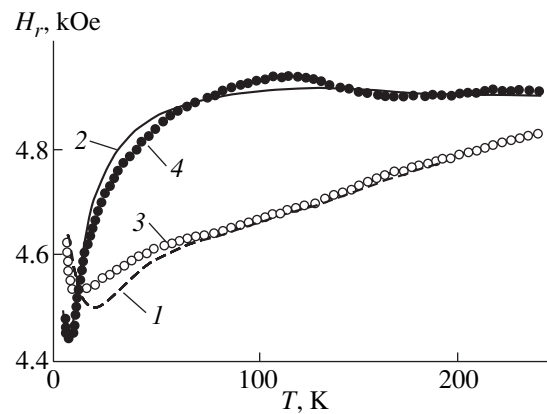


Fig. 2. Temperature dependences of the calculated (1, 2) and experimentally measured [4] (3, 4) resonance field for $\varphi = 0^\circ$ (1, 3) and $\varphi = 30^\circ$ (2, 4).

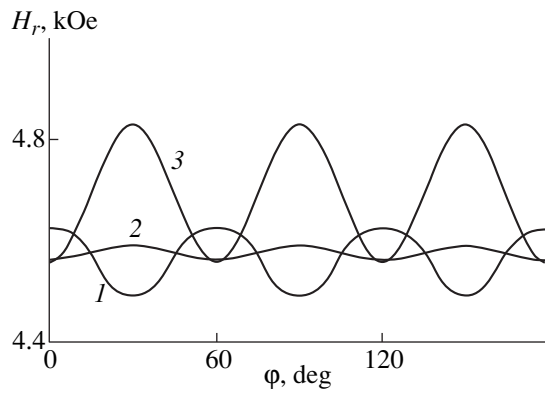


Fig. 3. Angular dependence of the resonance field for different temperatures T : 7 (1), 12 (2), and 36 K (3).

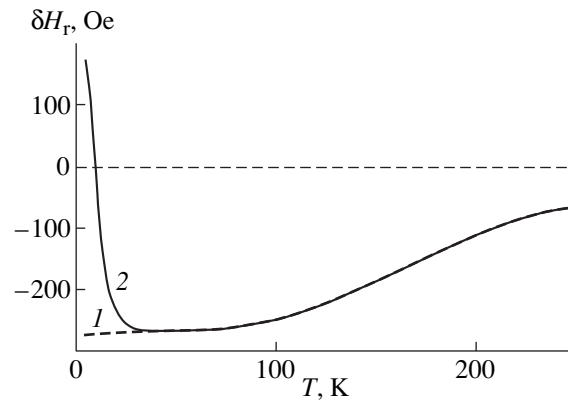


Fig. 4. Temperature dependence of the magnetic anisotropy field times $2H_E$ for a hematite crystal without an RE impurity (1) and doped with Dy^{3+} ions (2).

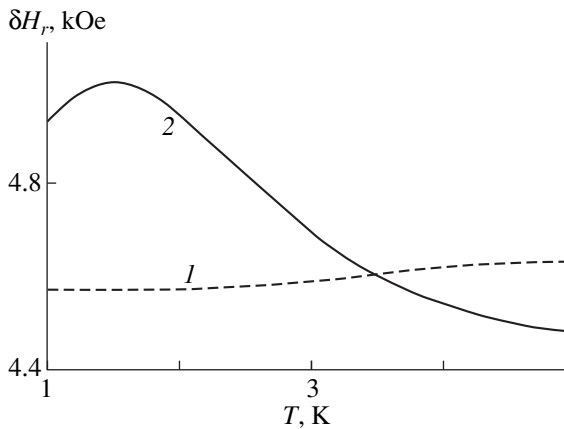


Fig. 5. Temperature dependences of the resonance field in the vicinity of a low-temperature anomaly for $\phi = 0$ (1) and $\phi = 30^\circ$ (2).

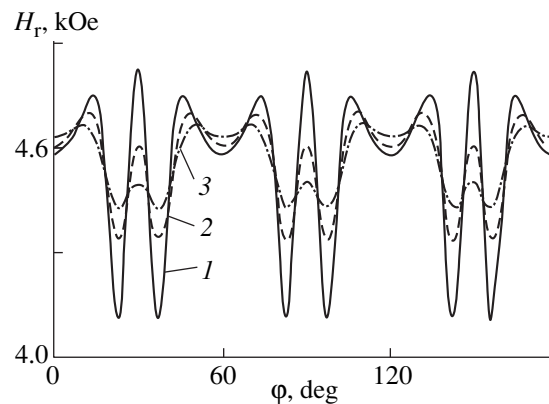


Fig. 6. Angular dependences of the resonance field for different temperatures T : 2.5 (1), 3.5 (2), and 4.5 K (3).

$H_{AB}(T)$ dependence for $\alpha\text{-Fe}_2\text{O}_3 : \text{Ga}$ (4 at. %) crystals, but the possible effect of Dy ions is not taken into account. Nonetheless, on the whole, the results also agree satisfactorily with the experiment in this case. The $\Delta(T)$ dependence is taken such that H_r at $\phi = 15^\circ$ is equal to the experimental values at $T = 7$ and 300 K. The dependence

$$\delta H_r(T) = H_r(T, \phi = 0) - H_r(T, \phi = 30^\circ), \quad (7)$$

which is frequently used in processing experimental data, may tell something about the temperature dependence of the magnetic anisotropy field (Fig. 4). It is seen from Fig. 4 that the contribution from the RE-ion subsystem becomes noticeable only at $T < 48$ K (curve 2), whereas the contribution from the crystal host dominates at higher temperatures (curve 1; cf. Fig. 1 in [4]). When expression (7) is used to process the data, it may appear that another spin-reorientational phase transition occurs at $T^* \cong 3.5$ K in this case (see Fig. 5), and

the easy magnetization axis has the same direction at $T < T^*$ and $T > T_{\text{ph}}$. However, analysis of the $H_r(T, \phi)$ angular dependence at different temperatures in the range $T < 5$ K (Fig. 6) reveals that this dependence is complicated and determined by the balance between the contributions from Dy ions at different inequivalent crystallographic positions. Therefore, in this case, there occurs a change in the character of the temperature dependence, rather than a change in the hard and easy magnetization directions.

4. CONCLUSION

This study established the cause and the features of the spin-reorientational phase transition that occurs in an $\alpha\text{-Fe}_2\text{O}_3 : \text{Ga}$ crystal with its doping with dysprosium. According to the model calculations, the low energy levels of impurity ions make the dominant contribution. Taking higher levels into account does not

alter the results radically, although the agreement with the experiment becomes better. The surprising thing is that, for the theoretical results to agree with the experimental data, the exchange interaction between RE ions and the Fe-ion subsystem must be taken to be of the ferromagnetic type, which is not typical of oxide compounds containing RE ions. This fact calls for further investigation.

APPENDIX I

$$\Psi_1 = 0.633 \left| \pm \frac{13}{2} \right\rangle - 0.582 \left| \pm \frac{5}{2} \right\rangle$$

$$- 0.451 \left| \mp \frac{3}{2} \right\rangle - 0.239 \left| \mp \frac{11}{2} \right\rangle$$

$$\mu_1 = \pm 2.83 \mu_B$$

$$\Psi_2 = -0.397 \left| \pm \frac{15}{2} \right\rangle - 0.398 \left| \pm \frac{11}{2} \right\rangle - 0.352 \left| \pm \frac{7}{2} \right\rangle$$

$$- 0.447 \left| \pm \frac{3}{2} \right\rangle + 0.458 \left| \mp \frac{1}{2} \right\rangle$$

$$- 0.125 \left| \mp \frac{5}{2} \right\rangle + 0.095 \left| \mp \frac{9}{2} \right\rangle - 0.354 \left| \mp \frac{13}{2} \right\rangle$$

$$\mu_2 = \pm 1.79 \mu_B$$

$$\Psi_3 = -0.396 \left| \pm \frac{15}{2} \right\rangle + 0.399 \left| \pm \frac{11}{2} \right\rangle - 0.352 \left| \pm \frac{7}{2} \right\rangle$$

$$+ 0.448 \left| \pm \frac{3}{2} \right\rangle + 0.458 \left| \mp \frac{1}{2} \right\rangle$$

$$+ 0.125 \left| \mp \frac{5}{2} \right\rangle + 0.095 \left| \mp \frac{9}{2} \right\rangle + 0.354 \left| \mp \frac{13}{2} \right\rangle$$

$$\mu_3 = \pm 1.79 \mu_B$$

$$\Psi_4 = 0.582 \left| \pm \frac{15}{2} \right\rangle + 0.331 \left| \pm \frac{7}{2} \right\rangle$$

$$+ 0.718 \left| \mp \frac{1}{2} \right\rangle + 0.191 \left| \mp \frac{9}{2} \right\rangle$$

$$\mu_4 = \pm 2.5 \mu_B$$

$$\Psi_5 = -0.047 \left| \pm \frac{15}{2} \right\rangle - 0.502 \left| \pm \frac{11}{2} \right\rangle + 0.03 \left| \pm \frac{7}{2} \right\rangle$$

$$+ 0.314 \left| \pm \frac{3}{2} \right\rangle - 0.164 \left| \mp \frac{1}{2} \right\rangle + -0.24 \left| \mp \frac{5}{2} \right\rangle$$

$$+ 0.705 \left| \mp \frac{9}{2} \right\rangle + 0.254 \left| \mp \frac{13}{2} \right\rangle$$

$$\mu_5 = \mp 1.26 \mu_B$$

$$\Psi_6 = -0.044 \left| \pm \frac{15}{2} \right\rangle + 0.53 \left| \pm \frac{11}{2} \right\rangle + 0.029 \left| \pm \frac{7}{2} \right\rangle$$

$$- 0.331 \left| \pm \frac{3}{2} \right\rangle - 0.155 \left| \mp \frac{1}{2} \right\rangle + 0.253 \left| \mp \frac{5}{2} \right\rangle$$

$$+ 0.668 \left| \mp \frac{9}{2} \right\rangle - 0.286 \left| \mp \frac{13}{2} \right\rangle$$

$$\mu_6 = \mp 0.92 \mu_B$$

$$\Psi_7 = -0.376 \left| \pm \frac{15}{2} \right\rangle + 0.232 \left| \pm \frac{11}{2} \right\rangle + 0.514 \left| \pm \frac{7}{2} \right\rangle$$

$$- 0.333 \left| \pm \frac{3}{2} \right\rangle + 0.076 \left| \mp \frac{1}{2} \right\rangle - 0.547 \left| \mp \frac{5}{2} \right\rangle$$

$$- 0.029 \left| \mp \frac{9}{2} \right\rangle + 0.353 \left| \mp \frac{13}{2} \right\rangle$$

$$\mu_7 = \pm 0.88 \mu_B$$

$$\Psi_8 = -0.449 \left| \pm \frac{15}{2} \right\rangle - 0.194 \left| \pm \frac{11}{2} \right\rangle + 0.614 \left| \pm \frac{7}{2} \right\rangle$$

$$+ 0.279 \left| \pm \frac{3}{2} \right\rangle + 0.09 \left| \mp \frac{1}{2} \right\rangle + 0.458 \left| \mp \frac{5}{2} \right\rangle$$

$$- 0.035 \left| \mp \frac{9}{2} \right\rangle - 0.295 \left| \mp \frac{13}{2} \right\rangle$$

$$\mu_8 = \pm 2.06 \mu_B$$

APPENDIX II

$$Z_{pq} = \cosh\left(\frac{E_{pq}^{(1)}}{T}\right) + 4 \exp\left(\frac{-E_{pq}^{(2)}}{T}\right),$$

$$F_{\Phi_1 \Phi_2} = \sum_{\{pq\}} \left\{ \frac{\partial^2 E_{pq}^{(1)}}{\partial \Phi^2} \frac{\sinh(E_{pq}^{(1)}/T)}{Z} + \frac{8}{T} \left[\left(\frac{\partial E_{pq}^{(1)}}{\partial \Phi} \right)^2 \right. \right. \\ \left. \left. + \frac{1}{2} E_{pq}^{(1)} \frac{\partial^2 E_{pq}^{(1)}}{\partial \Phi^2} \right] \frac{1 + \cosh(E_{pq}^{(1)}/T) \exp(-E^{(2)}/T)}{Z^2} \right. \\ \left. - \frac{4}{T^2} E_{pq}^{(1)} \left(\frac{\partial E_{pq}^{(1)}}{\partial \Phi} \right)^2 \frac{\sinh(E_{pq}^{(1)}/T) \exp(-E^{(2)}/T)}{Z^2} \right. \\ \left. - \frac{8}{T^2} E_{pq}^{(1)} \left(\frac{\partial E_{pq}^{(1)}}{\partial \Phi} \right)^2 \right. \\ \left. \times \frac{[1 + \cosh(E_{pq}^{(1)}/T) \exp(-E^{(2)}/T)] \sinh(E_{pq}^{(1)}/T)}{Z^3} \right. \\ \left. + \frac{2}{T} E^{(2)} \frac{\partial^2 E_{pq}^{(2)}}{\partial \Phi^2} \frac{\sinh(E^{(2)}/T) \exp(-E^{(2)}/T)}{Z^2} \right. \\ \left. - \frac{2}{T^2} E^{(2)} \left(\frac{\partial E_{pq}^{(1)}}{\partial \Phi} \right)^2 \frac{\exp(-E^{(1)}/T)}{Z^2} \right. \\ \left. \times \left[\cosh(E_{pq}^{(1)}/T) - \frac{2 \sinh^2(E_{pq}^{(1)}/T)}{Z} \right] \right\}$$

REFERENCES

1. A. K. Zvezdin, V. M. Matveev, A. A. Mukhin, and A. I. Popov, *Rare-Earth Ions in Magnetically Ordered Crystals* (Nauka, Moscow, 1985).
2. V. N. Vasil'ev and E. N. Matveiko, in *Physical Properties of Ferrites* (Inst. Fiz. Sib. Otd. Akad. Nauk SSSR, Krasnoyarsk, 1987), p. 46.
3. G. S. Patrin, N. V. Volkov, and V. N. Vasiliev, *Phys. Lett. A* **230**, 96 (1997).
4. G. S. Patrin, N. V. Volkov, and E. V. Eremin, *Pis'ma Zh. Éksp. Teor. Fiz.* **63** (12), 941 (1996) [*JETP Lett.* **63**, 725 (1996)].
5. S. Geschwind and J. P. Remeika, *Phys. Rev.* **122** (3), 757 (1961).
6. E. J. Samuelsen and G. Shirane, *Phys. Status Solidi* **42**, 241 (1970).
7. A. G. Gurevich, *Magnetic Resonance in Ferrites and Antiferromagnets* (Nauka, Moscow, 1973).
8. E. F. Kustov, G. A. Bondurkin, É. N. Murav'ev, and V. P. Orlovskii, *Electronic Spectra of Rare-Earth Compounds* (Nauka, Moscow, 1981).
9. K. R. Lee, M. J. Leask, and W. P. Wolf, *J. Phys. Chem. Solids* **23** (10), 1381 (1962).
10. P. Grunberg, S. Hufner, E. Orlich, and J. Schmitt, *J. Appl. Phys.* **40** (3), 1501 (1969).

Translated by Yu. Epifanov